Automated Energy Storage and Curtailment System to Mitigate Distribution Transformer Aging due to High Renewable Energy Penetration

Humberto Queiroz[a,b,*], Rui Amaral Lopes[a,b], João Martins[a,b]

[a]*Faculty of Sciences and Technology – NOVA University of Lisbon, Portugal*
[b]*Center of Technology and Systems (CTS) - UNINOVA, Portugal*

Abstract

The increase of distributed generation units in low voltage distribution grids, stimulated by different mechanisms (mostly economic), like the Energy Performance of Buildings Directive in Europe and the associated nearly-Zero Energy Building concept, stresses in-depth research on the possible impacts that such generation may impose on fundamental grid equipment such as distribution transformers.

Taking this into consideration, this paper has two main objectives: i) to analyze the impacts of distributed generation on a non-residential building supplied by a dedicated distribution transformer when this building is converted to a nearly-Zero Energy Building; and ii) to develop a Transformer Anti-Aging Protection System (TAAPS) that mitigates existing negative impacts in order to reduce transformer aging.

The present study is based on 1-year, 1-min resolution, real electricity demand and weather data and uses the standard IEC 60076-7 (Loading Guide For Oil-immersed Power Transformers) to model the transformer aging. The collected results show that the introduction of distributed generation increases transformer aging and that the proposed protection system (TAAPS) fulfills its objectives preventing the excessive aging. An economic analysis, related with the proposed system, is also provided in this paper.

Keywords: Photovoltaic systems, Distribution transformer, Energy storage, Generation curtailment.

* Corresponding author. Tel.: +351 212947876
E-mail address: h.queiroz@campus.fct.unl.pt

1 – Introduction

Due to technological and economic advances, humanity has witnessed an increase in energy consumption of all its forms [1]. Since the main source of energy supply is still fossil fuels, energy consumption has contributed to increase the concentration of Greenhouse Gases (GHG) in the atmosphere in the last decades [1], with the main negative impact being pointed out as the resulting Earth's surface average temperature increase and related phenomena [2]. In this context, Renewable Energy Sources (RES) play an important role in near future energy systems due to their often GHG emission-free operation, being their integration into power systems encouraged worldwide (see, for instance, the Kyoto Protocol [3] or the Paris Agreement [4]). Additionally, on the demand side, energy efficiency improvements are referred to as an important part of the solution [5,6].

Taking the particular case of Europe into consideration, where buildings alone are responsible for 40% of the energy consumption and 36% of CO_2 emissions [7], the nearly Zero-Energy Building (nZEB) concept has been introduced, in 2010, by the Performance of Buildings Directive (EPBD) recast aiming to increase both the energy efficiency of European building stock and the integration of RES at local level. As referred by the respective directive [8], nZEBs should present low energy demand, due to their high energy efficiency, and be able to cover their energy needs mostly using RES based conversion systems located on-site or nearby. While many different technologies can be used to convert energy on-site, most nZEBs rely on solar photovoltaic (PV) systems [9]. Therefore, since PV systems present a generation profile dependent on the solar resource availability, the majority of nZEBs are connected to power grids and rely on them to import energy when on-site generation is not available or to export energy when a generation surplus is registered. In fact, over a certain period of time (typically one year),

nZEBs usually presents net-zero energy balances, exporting as much energy to power grids as they import [10].

Despite all the advantages of using RES in nZEBs, or in other types of buildings, it is important to note that at some periods generation may not be correlated with demand and that large amounts of energy may be exported to power distribution grids that were not originally designed to accommodate such reverse power flows [11–14]. Being distribution transformers one of the most important components integrating these grids [15], the impacts introduced on their operation and aging should be carefully analyzed. The literature shows that these impacts, imposed by the modification on the distribution grids' power flows, can be both positive and negative, depending on the RES integration level [16–29]. More specifically, low RES integration levels result on positive impacts on distribution transformers' operation and aging due to the reduction of the power flows' magnitude [16–24], while high RES integration levels may conduct to negative impacts due to reverse power flows whose magnitude cannot be supported by the distribution transformers under consideration [23–29]. However, the literature is still lacking studies focused on distribution transformers suppling large single buildings, which is the case when energy supply is conducted at medium voltage, but the respective electricity demand occurs at low voltage levels, as it is common in large non-residential buildings. Additionally, studies addressing the development and assessment of automated systems to protect distribution transformers in case of excessive reverse power flows are still missing.

Taking this into consideration, the contribution of the study described in this paper is twofold. Firstly, the impacts of RES on a distribution transformer supplying a single large non-residential building are studied. Then, a Transformer Anti-Aging Protection System (TAAPS), developed to mitigate negative impacts introduced on the transformer's

operation and aging by reverse power flows, is presented and assessed. This TAAPS, designed to be used in non-residential buildings with dedicated transformers, uses the energy flexibility offered by a Battery Energy Storage System (BESS) and/or a curtailment mechanism to limit transformer aging. One non-residential building located in Lisbon area, Portugal, is used as case study and 1-min resolution real data of energy consumption and weather conditions, collected throughout an entire year, are considered. This paper is structured as follows; Section 2 presents the methodology used in this study, describing the electrical energy consumption of the building and the used meteorological data, the considered PV system and the system developed to protect the distribution transformer from the accelerated aging (i.e. the TAAPS); Section 3 focus the results obtained for different scenarios related with the building operation (before its transition to nZEB, after this transition and considering the TAAPS); and Section 4 provides the conclusions of this study and possible future work.

2 – Methodology

The assessment of the impacts originated by the conversion of a non-residential building into nZEB is based on the validated model described in the IEC 60076-7 (Loading Guide For Oil-immersed Power Transformers) [30] and on real data associated to the building's energy demand, outside ambient temperature and registered global solar irradiance for the entire year of 2013. The building under analysis is the home of the Department of Electrical and Computer Engineering of the Faculty of Sciences and Technology of Nova University of Lisbon, in Portugal. The load profile of the building is described in Section 2.1 while the model used to simulate the PV generation profile is described in Section 2.2, together with the method followed to size the number of PV modules needed to match the energy balance of the nZEB condition. Then, Section 2.3 describes the proposed

TAAPS and provides information on the thermal behavior and resulting aging of the distribution transformer.

2.1 – Electricity demand profile

The Faculty of Sciences and Technology campus has an area of more than 30 ha with 14 large buildings. The campus has its own medium voltage grid (15 kV) with 12 distribution transformers. In particular the building of the Department of Electrical and Computer Engineering (DEEC) is supplied by one of those distribution transformers. It is important to note that, at the time of the building construction, no concerns were considered in the transformer design. Therefore, for the specific purpose of this study, the sizing of the transformer was conducted in order to ensure that the instantaneous load is never higher than 1.5 times the rated load, as recommended by the IEC 60076-7 for a normal cycle loading [30]. Table 1 presents the main characteristics of the considered distribution transformer (DT). Regarding other energy carriers influencing the building's energy demand, an oil boiler heating system is used to satisfy the existing heating needs.

Table 1 – Parameters of the Department of Electrical and Computer Engineering's distribution transformer.

Rated Power	Transform Relation	Insulation	Cooling
124 kVA	15 kV - 0,4/0,23 kV	Oil immersed	ONAN

Figure 1 presents the electricity demand profile of the building (with 1-min resolution) for the entire year of 2013, where the dashed red line represents the DT's limit load for a normal operation. This figure also presents the daily average load (black line), which exhibits higher values during summer due to the operation of the HVAC system used to satisfy the cooling demand. Throughout this paper all figures presenting values related to

the building's electricity demand and/or generation are normalized to DT's rated load (i.e. 124 kVA).

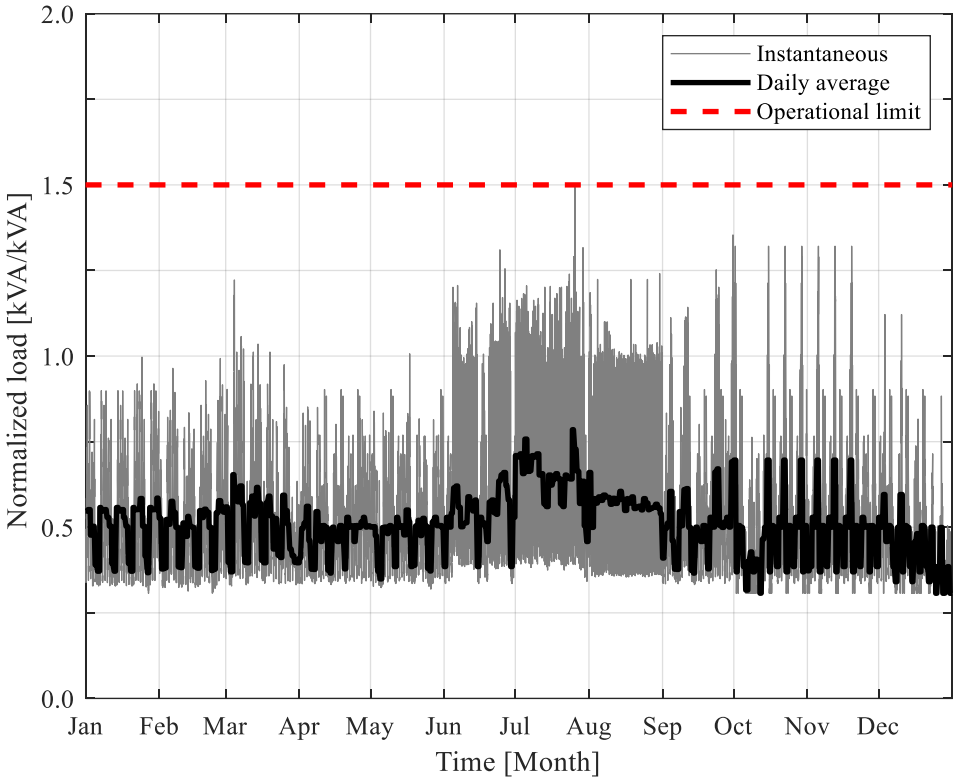

Figure 1 – Instantaneous and daily average building's load profile, normalized to DT's rated load.

2.2 – Electricity generation profile

To convert the DEEC building to nZEB, a PV system is considered for installation to generate on-site energy. The annual electricity consumption E_C is taken into consideration to size the rated power of this PV system so that the building generates as much on-site electricity, E_G, as the building consumes over a 1-year period (E_C). E_G depends on the number of PV modules (N) and on the annual generation of each module (E_M), as described by Equation 1, assuming that all modules perform equally. Therefore, in this case, the number of PV modules necessary to convert the building to nZEB is given by Equation 2.

$$E_G = N \times E_M \quad (1)$$

$$N = \frac{E_C}{E_M} \quad (2)$$

$$P_G(n) = N \times P_M(n) \quad (3)$$

For a single PV module, the power output is described in Equation 4 [31], where A is the total area of a PV module, $G(n)$ is the instantaneous global solar irradiance at the considered local, $\eta_c(n)$ is the instantaneous PV module's efficiency, given by Equation 5, and η_i is the efficiency of the converting power electronics equipment (e.g. DC/AC inverter).

$$P_M(n) = A \times G(n) \times \eta_c(n) \times \eta_i \quad (4)$$

$$\eta_c(n) = \eta_{STC} \times \left\{1 + \mu \times \left[\theta_a(n) - T_{c,STC} + G(n) \times \left(\frac{T_{c,NOCT} - \theta_{a,NOCT}}{G_{NOCT}}\right) \times (1 - \eta_{STC})\right]\right\} \quad (5)$$

In Equation 5, η_{STC} is the PV module's efficiency at Standard Test Conditions (STC), μ is the temperature coefficient, $\theta_a(n)$ is the ambient temperature, $T_{c,STC}$ is the cell temperature at STC, $T_{c,NOCT}$ is the cell temperature at NOCT, $\theta_{a,NOCT}$ is the ambient temperature at Nominal Operating Cell Temperature (NOCT) and G_{NOCT} is the global irradiance at NOCT. The PV system related parameters used in this study are presented in Table 2, while the values of $\theta_a(n)$ and $G(n)$ are showed in Figure 2. The ambient temperature and the global irradiance for the horizontal plan were collected with 1-min resolution by a weather station located at the DEEC building. While the ambient temperature values were directly used in this study, the global irradiance values were transferred to a 33º tilt plan before being used. This is the angle that maximizes the PV

annual energy generation of a single module in the location of the considered building, being the respective transfer performed according to the geometric factor described in [32].

Table 2 – Parameters of the PV module used to size the PV system.

Parameter	Value	Unit
A	1	m^2
η_i	0.9	-
η_{STC}	0.15	-
μ	-0.0045	$^oC^{-1}$
$T_{c,STC}$	25	^oC
$T_{c,NOCT}$	47	^oC
$\theta_{a,NOCT}$	20	^oC
G_{NOCT}	800	$W.m^{-2}$

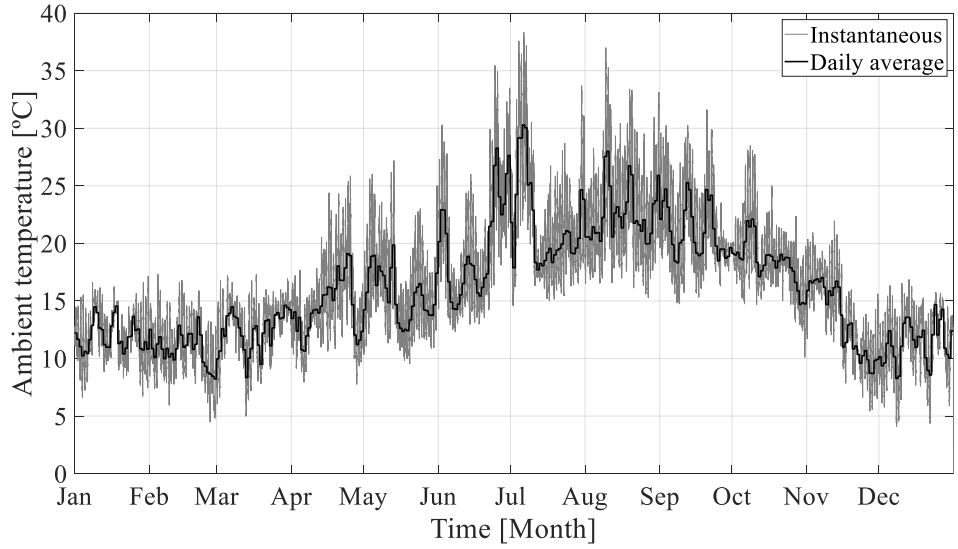

(a)

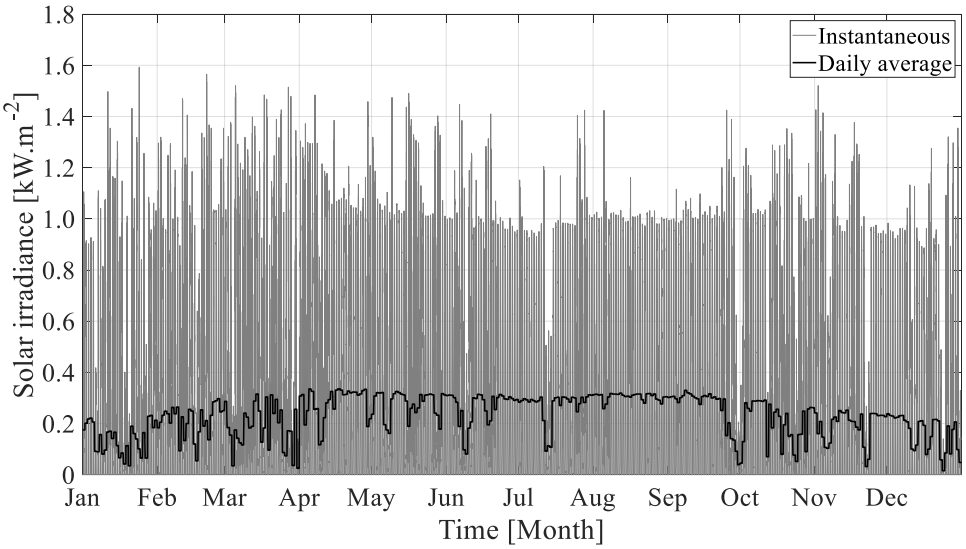

(b)

Figure 2 – Weather data used in this study (1-min resolution): (a) Ambient temperature. (b) Global solar irradiance at 33º tilt plan.

2.3 – Transformer Anti-Aging Protection System

In order to avoid transformer's excessive aging due to the reverse power flows originated by the introduction of on-site PV generation, the Transformer Anti-Aging Protection System (TAAPS) is design to use (i) a BESS, (ii) a combination of a BESS and generation curtailment or (iii) only generation curtailment. Therefore, the TAAPS main objective is to define, at each time-step n, the needed power for the charging and discharging cycles

of the BESS (B) and/or the level of power curtailment of the PV matrix (Cm) as a function of the transformer load and its associated insulation oil temperature. Since both the oil and winding temperature are not equally distributed, IEC 60076-7 [30] defines two critical temperatures that affect the transformer's operating conditions: the top-oil temperature θ_o and the hotspot temperature θ_h. The top-oil temperature is defined as the hottest point of the oil in the transformer's tank while the hotspot temperature refers to the hottest point of the insulating oil inside the transformer's windings, which, by default, is higher than the top-oil temperature to a considered load due to current flowing on the windings. The hotspot temperature is obtained using the model described in the IEC 60076-7 and used to compute the transformer aging [30]. To achieve this objective, TAAPS operation is based on three main modules (presented in Figure 3): i) Data Acquisition Module; ii) Control Module; and iii) Interface Module.

The **Data Acquisition Module** aims to collect, at each time-step, all the variables needed for a proper system operation. These variables are the ambient temperature (θ_a), the top-oil temperature of the transformer (θ_o), in case the transformer provides this information, the building's electricity demand (D), the power generated by the PV matrix (P_G) and the BESS state-of-charge (SoC). The **Control Module** is responsible for computing the maximum admitted load for the transformer to not exceed its hotspot temperature (θ_h) operational limit of 140ºC[1] while ensuring that this load is lower than 1.5 times the transformer's rated load. Then, taking into consideration the current load and this maximum load value, the Control module computes the value of B, Cm and the resulting

[1] According to [30], if the hotspot temperature exceeds 140ºC gas bubbles may occur in the insulation oil which can compromises the dielectric strength of the transformer.

θ_h during the considered time-step. The **Interface Module** displays all the collected and calculated variables for the system user.

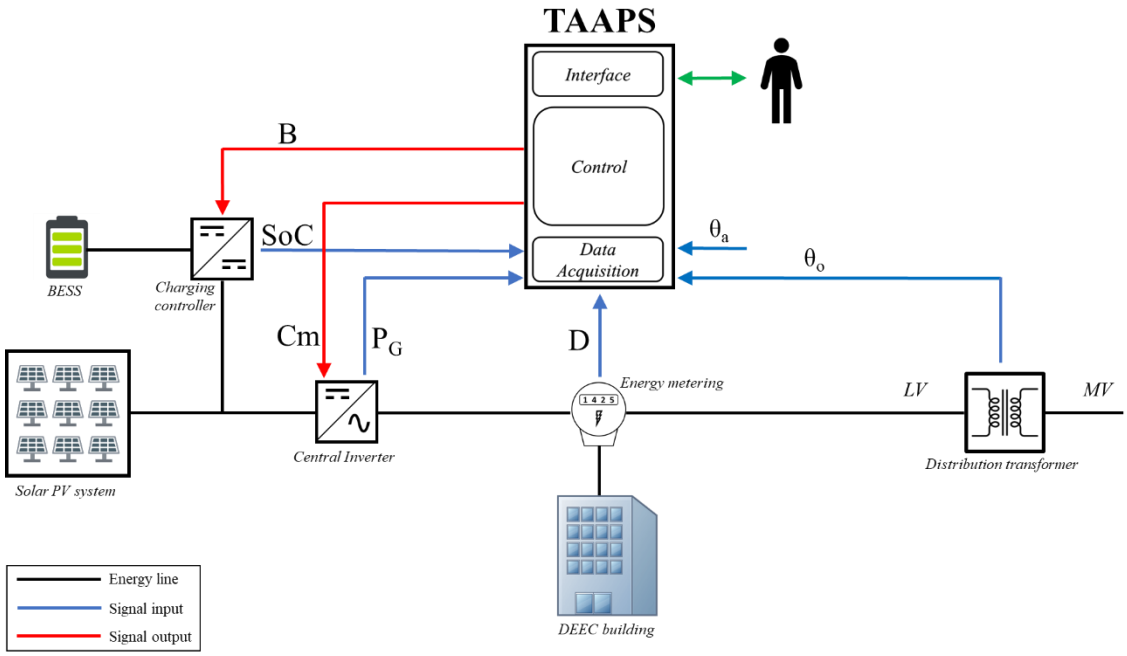

Figure 3 – Schematic of the TAAPS.

Given the importance of the Control Module for the TAAPS operation, the next sections provide a detail description of the considered models and algorithms. Namely, Section 2.3.1 describes the thermal behavior model of the transformer, Section 2.3.2 explains the aging process of the transformer and Section 2.3.3 shows the algorithms used to prevent the transformer from excessive aging.

2.3.1 – Transformer thermal behavior

According to IEC 60076-7 [30], the hotspot temperature can be mathematically described, for varying load and ambient temperature, by a series of differential equations related to heat transfer processes. However, in order to make it applicable for online monitoring, these differential equations can be transformed into difference equations in

which the outputs of the $(n-1)$ timestep are inputs for the n timestep. Figure 4 presents the block diagram of the thermal process described by these difference equations. The input variables are the instantaneous load applied to the transformer terminals normalized to the rated power, usually defined as load factor (Equation 6), and the ambient temperature (θ_a).

$$K_L = |(D - P_G)|/L_R \quad (6)$$

As shown in Figure 4, if the top-oil temperature is measured then the alternative path defined by the dashed line can be used and the ambient temperature is no longer a required input. Table 3 describes the parameters and associated values used in this study, which were obtained from IEC 60076-7 [30] and refer to the DEEC distribution transformer.

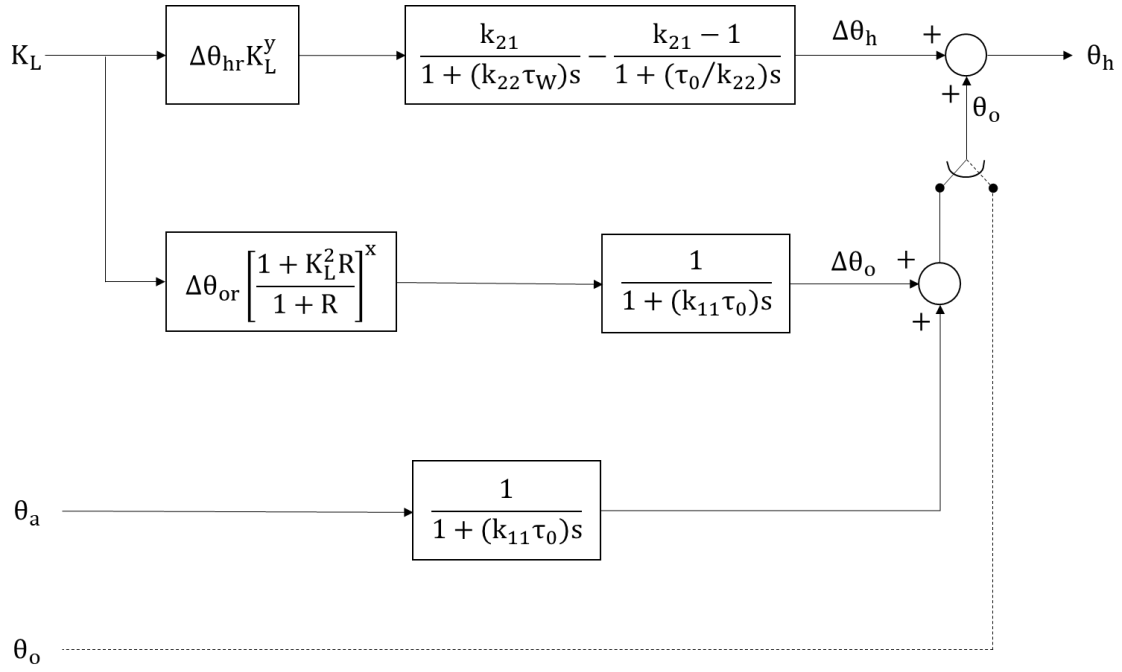

Figure 4 – Differential equations' blocks diagram of the transformer's thermal behavior [30].

Table 3 – Description and values of the transformer's thermal model parameters [30].

Constant	Description	Value
$\Delta\theta_{hr}$	Hot-spot-to-top-oil (in tank) gradient at rated current	35 K
$\Delta\theta_{or}$	Top-oil (in tank) temperature rise in steady state at rated losses (no-load losses + load losses)	45 K
k_{11}	Thermal model constant	1
k_{21}	Thermal model constant	1
k_{22}	Thermal model constant	2
L_R	Transformer rated power	124 kVA
R	Ratio of load losses at rated current to no-load losses	8
τ_o	Average oil time constant	180 min
τ_w	Winding time constant	4 min
x	Exponential power of total losses versus top-oil (in tank) temperature rise (oil exponent)	0,8
y	Exponential power of current versus winding temperature rise (winding exponent)	1,6

2.3.2 – Aging process

According to IEC 60076-7 [30], the aging process of a transformer (due to the deterioration of its insulating material) is a time function of temperature, moisture, oxygen and acid content of the insulating oil. Since the temperature distribution is not uniform in the tank, the part that operates at higher temperature (i.e. hotspot temperature) is submitted to greater deterioration and, according to [30], define the transformer relative aging rate (RAR), as described by Equation 7. Thereby, the equivalent Loss of Life (LOL) over a period defined by n_1 and n_2 is given by Equation 8. The term "equivalent" is used because RAR is computed against a reference scenario where the transformer has unitary aging when the $\theta_h = 110$ ºC whose results were experimentally obtained [30]. Therefore, hotspot temperatures higher/lower than 110 ºC originate RAR values higher/lower than one.

$$\mathrm{RAR(n)} = e^{\left(\frac{15.000}{110+273} - \frac{15.000}{\theta_h(n)+273}\right)} \quad (7)$$

$$\mathrm{LOL} = \sum_{n_1}^{n_2} \mathrm{RAR(n)} \quad (8)$$

2.3.3 – TAAPS control algorithms

To limit the power at the transformer terminals within the limits defined in terms of hotspot temperature and load, the Control Module uses two main algorithms. The first one is used to compute, at a specific time-step, the maximum power that can be applied at the transformer terminals during the next time-step in order to respect the load and hotspot temperature limits. In this case, the Control Module assumes that the ambient temperature does not change significantly between two time-steps and uses the thermal model shown in Figure 4 backwards, following an iterative approach, to find the K_L for the next time-step that originates a hotspot temperature of 140 ºC (i.e. the maximum allowed load) while being lower than 1.5 times the transformer's rated load. The flowchart that describes this algorithm is shown in Figure 5, referring the required input variables (i.e. maximum hotspot temperature ($\theta_{h,max}$), maximum load ($K_{L,max}$) and ambient temperature associated to the current time-step) and the desired output variable (i.e. the maximum load factor admitted in the transformer for the next time-step ($K_{L,max}$)).

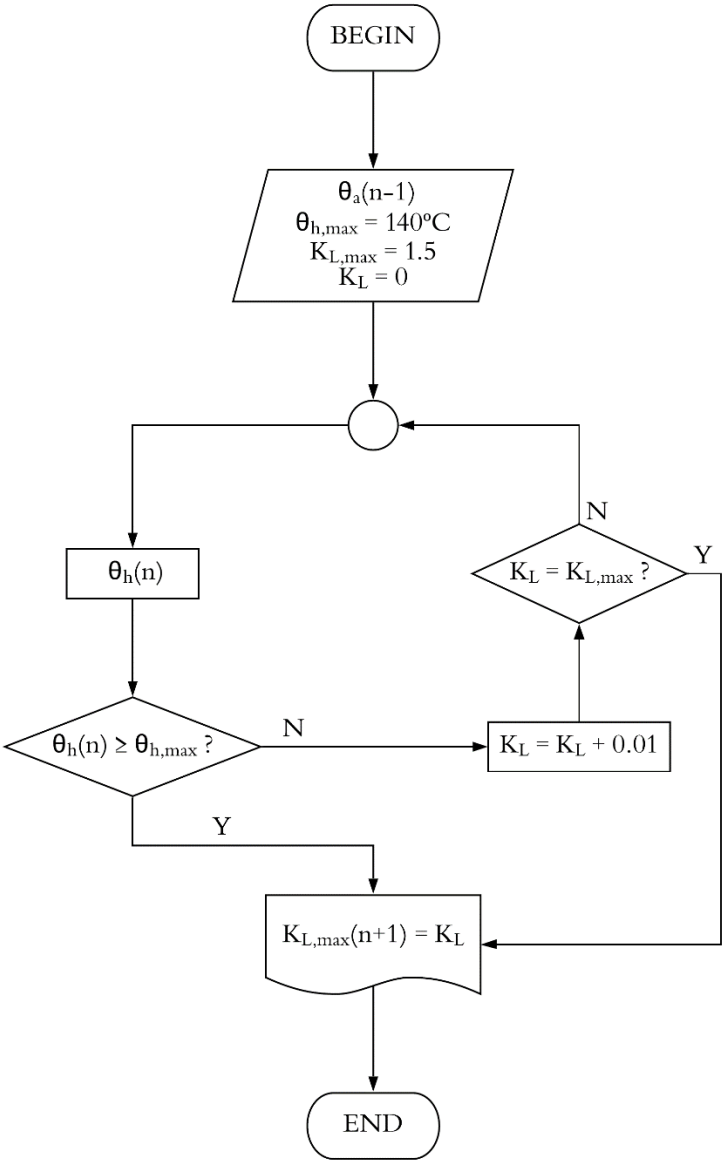

Figure 5 – Flowchart for the TAAPS maximum load prediction algorithm.

After computing the maximum load admitted for next time-step, the second algorithm defines the BESS charging (B) and/or the generation curtailment (Cm) in case of transformer overloading. In this case, the Control Modules can consider three different scenarios: i) the BESS is capable of storing all the energy needed to reduce the load to the maximum allowed value; ii) the BESS is not able to store all the energy and the remaining load reduction is ensured by the curtailment mechanism; and iii) there is no BESS and all the excessive load is mitigated by curtailment. Additionally, this algorithm

297 also establishes the BESS discharging when the building's electricity demand is higher
298 than its generation. The flowchart that describes this second algorithm is shown in Figure
299 6. In this case the input variables are the maximum load admitted, ($K_{L,max}$), which is
300 calculated at the previous timestep by the first algorithm, and the state of charge of the
301 BESS (SoC), also measured at the previous timestep by the Data Acquisition Module.
302 The remaining variables of interest for this second algorithm are described in Table 4.
303

304 *Table 4 – Interest variables and respective units for the TAAPS protection algorithm.*

Variable	Unit	Description
L	kW	Load at the transformer's output before the TAAPS operation, which is given by the difference between the building's demand and generation.
D	kW	Building's demand (see Figure 1).
P_G	kW	Building's generation (see Section 2.2)
CAP	kWh	Energy storage capacity of the BESS. If no BESS is used CAP is zero and TAAPS relies only on the curtailment mechanism to limit the transformer's load.
L_R	kW	Transformer's rated load (124 kVA in this study).
B	kW	Power at the BESS output.
α_T	W/kWh	Constant used to compute the energy storage at a specific time-step given the respective BESS power. In this study, $\alpha_T = 60000$ W/kWh since 1-min resolution data is used.
Cm	KW	Generation curtailment.
LOAD	KW	Load at the transformer's out after the TAAPS operation, which ensures $\theta_h <$ 140 ºC and transformer's load lower than its rated value.

305

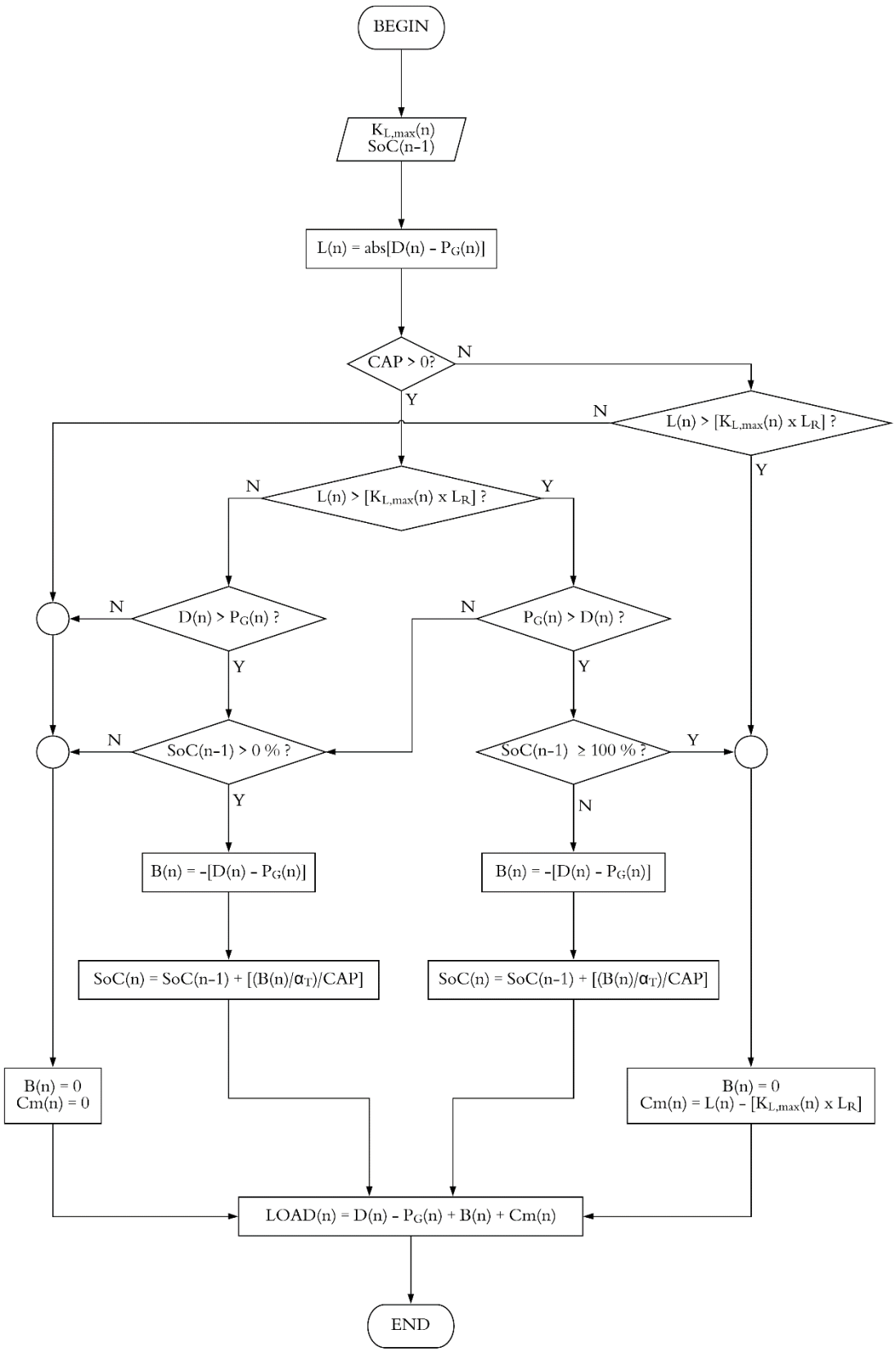

306
307 *Figure 6 – Flowchart for the TAAPS protection algorithm.*

308

3 – Results and analysis

To collect the results needed to assess the aging process of the transformer under analysis, throughout a year, three distinct scenarios are considered. The first scenario refers to the operation of the DEEC building before its conversion to nZEB, being the transformer's load always lower than 1.5 times the rated load. In the second scenario it is assumed that the building is converted to nZEB using a PV system large enough to compensate the annual electricity demand of the building. The last scenario regards the operation of the building with the proposed Transformer Anti-Aging Protection System, using energy storage and/or generation curtailment.

3.1 – Original DEEC building

In this scenario, the energy flowing through the transformer is only due to the demand of the building's electrical equipment, being the respective load profile shown in Figure 1. Based on the transformer thermal model, the top oil and hotspot temperature profiles are presented in Figure 7, while the equivalent aging calculated for the same period of analysis (1-year period) is shown in Figure 8.

In this case, over the 1-year period, the transformer suffers an equivalent aging of only 3 days. This reduced value results from the fact that the transformer was oversized for most of the analyzed year in order to respect the assumption followed to define the normal operation (i.e. transformer's load always lower than 1.5 the rated load). Therefore, most of the aging occurs during the summer, mainly due to the chiller's operation and higher ambient temperature, but still with a relatively low value. During the second part of the year Figure 8 presents higher equivalent aging due to the influence of the increased ambient temperature values that influence the hotspot temperature and the operation of the chiller. It is important to note that according to the conducted transformer sizing the

hotspot temperature never exceeds the value of 140ºC and that, as presented in Figure 1 (see Section 2.1), the transformer's load is always lower than 1.5 times its rating load. The transformer would have achieved an equivalent aging of 365 days if the hotspot temperature was kept equal to 110 ºC during the entire year.

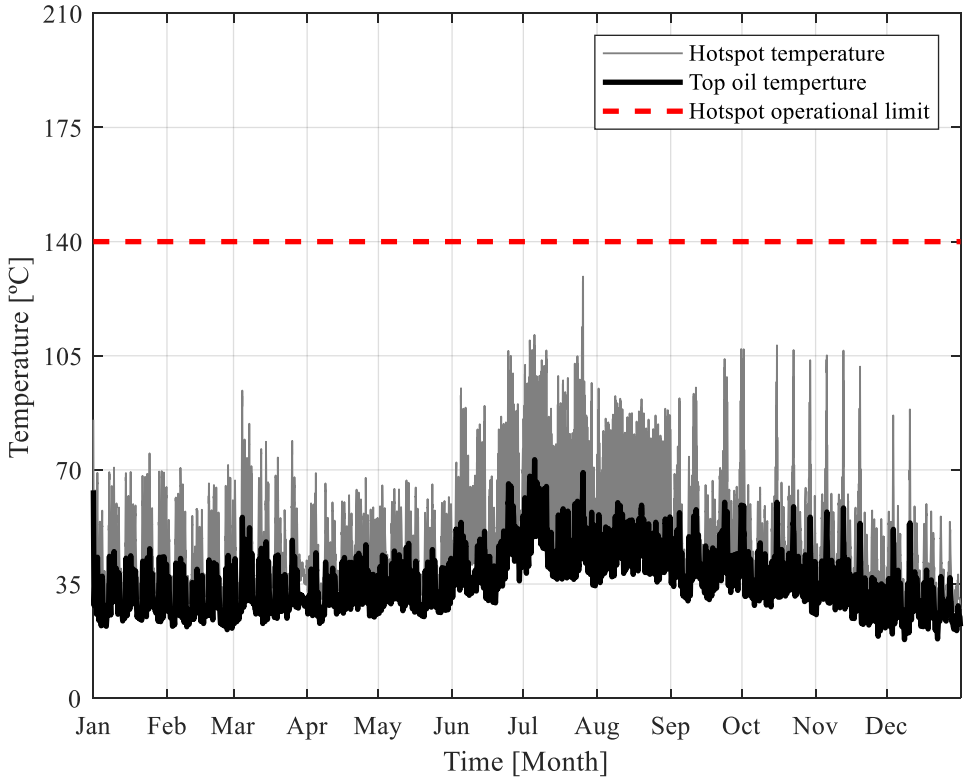

Figure 7 – Transformer temperature profiles without PV generation.

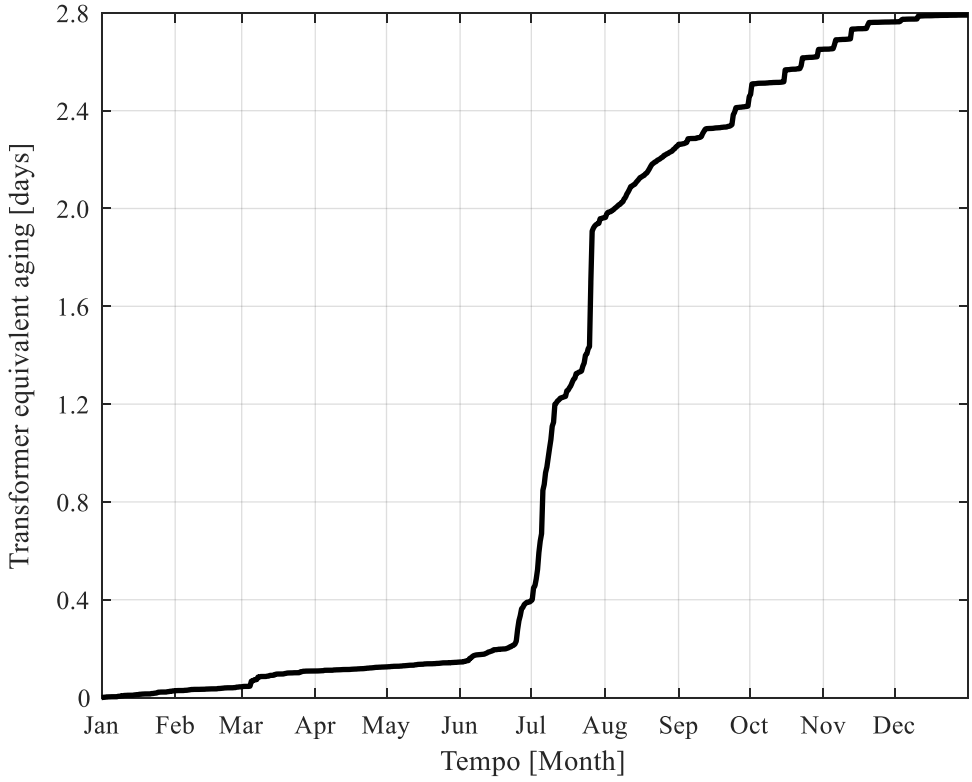

Figure 8 – Transformer equivalent aging without PV generation.

3.2 – DEEC building converted to nZEB

Due to the generation of the PV system, the conversion of the DEEC building to nZEB has a considerable impact on the load profile to which the transformer is subject. Figure 9 presents this generation for the analyzed year, where a maximum generation peak of 364 kW is observed. Figure 10 shows the resulting load profile imposed at the transformer. Since the nZEB relies on the solar resource to generate energy on-site, reverse power flows with a magnitude much higher than the original demand peaks are registered. As a result, the transformer no longer operates within the limits defined for its normal operation and reverse power flows with a magnitude of 2.65 times higher than the transformer's rated load can be found.

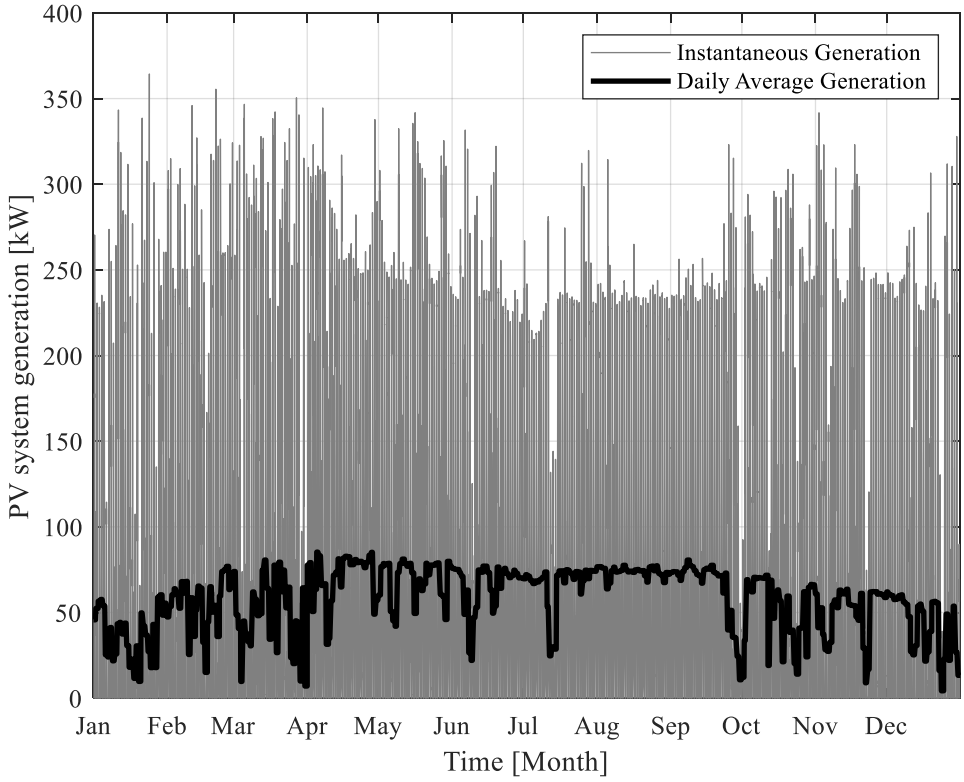

354
355 *Figure 9 – Generation profile of the PV system*

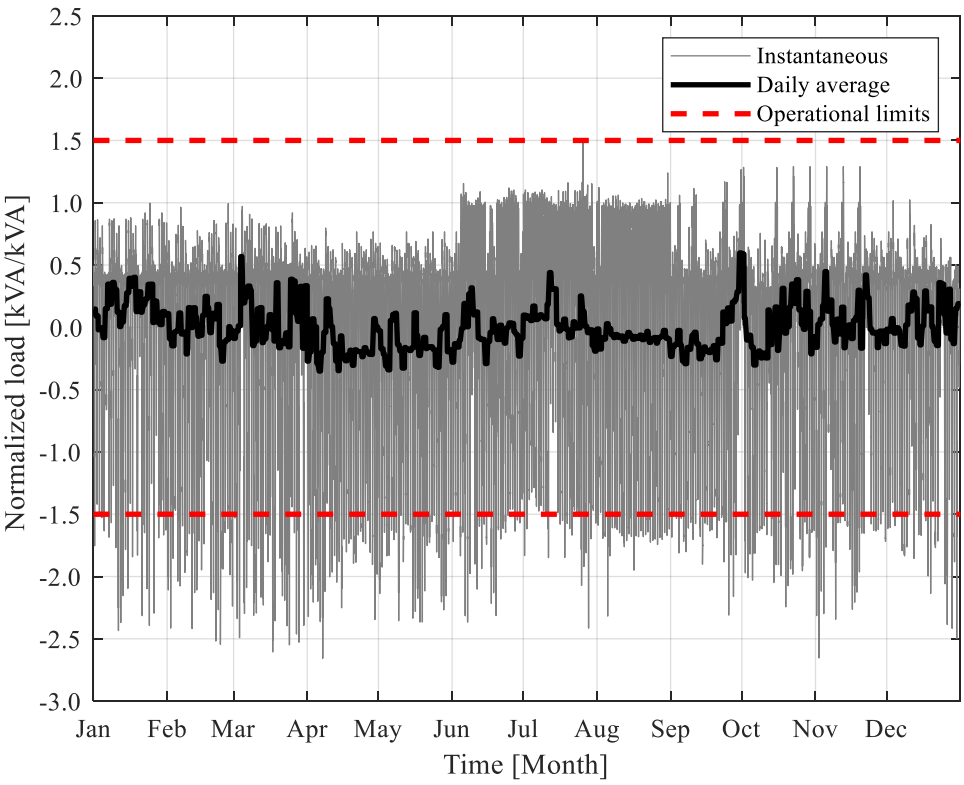

356
357 *Figure 10 – Instantaneous and daily average load profile of the transformer at the nZEB*
358 *condition.*

Regarding the top oil and hotspot temperatures, which are presented in Figure 11, these are also deeply impacted by the PV generation and associated reverse power flows, reaching maximum values of 107 ºC and 204 ºC, respectively. Such high temperatures would probably conduct to the transformer failure as it can also be observed by the equivalent aging for the analyzed period. Figure 12 shows the equivalent aging throughout the entire year. In this case, the equivalent aging of the transformer is 2050 days, reflecting a hotspot temperature higher than 110 ºC during a significant amount time.

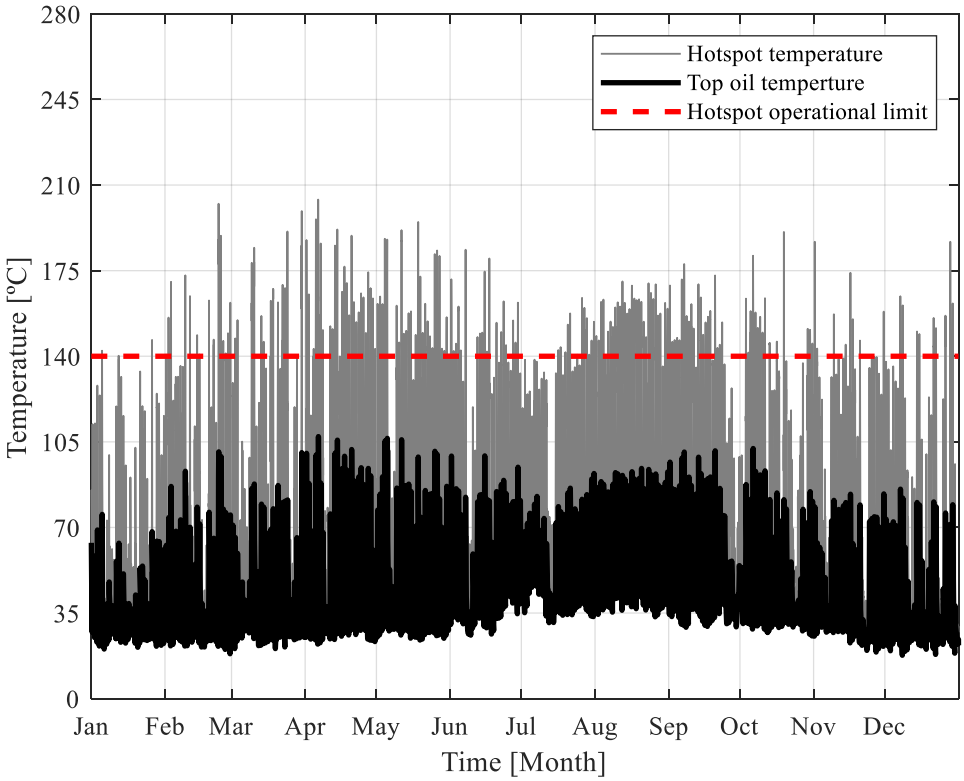

Figure 11 – Transformer temperature profile when the building is converted to nZEB.

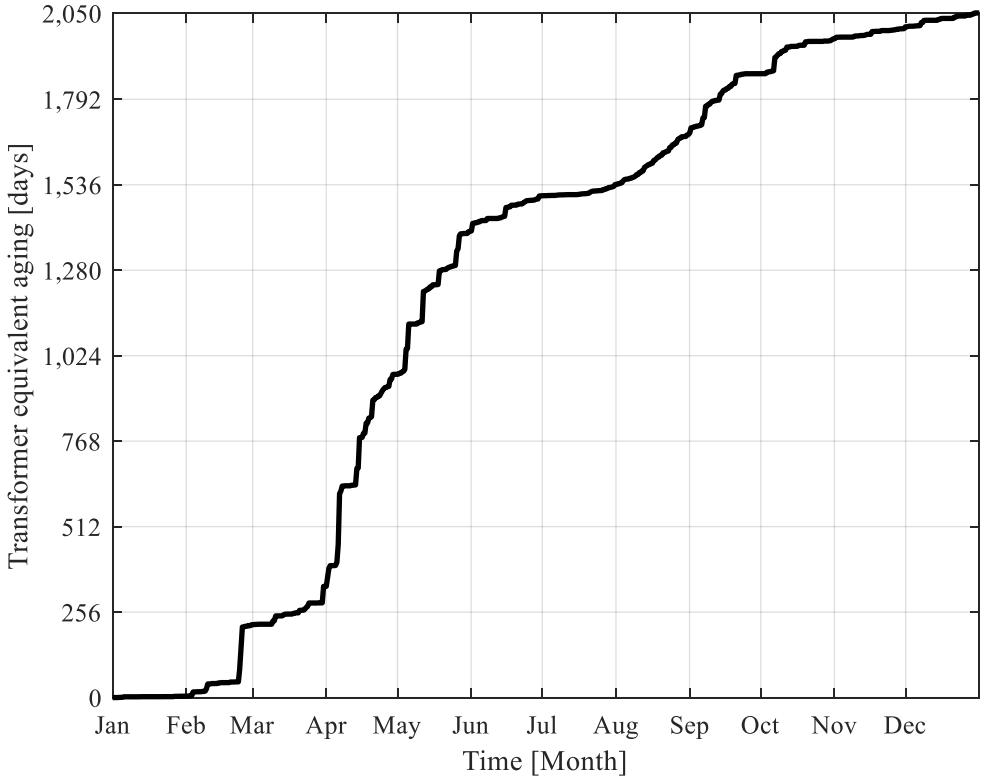

Figure 12 – Transformer equivalent aging at the nZEB condition.

3.3 – nZEB equipped with the Transformer Anti-Aging Protection System

To mitigate the negative impacts introduced by the reverse power flows observed after the conversion of the original building to nZEB (see Section 3.2), the proposed TAAPS is used and the respective results are presented and analyzed in this section. It is assumed that TAAPS uses BESS, BESS and curtailment (BESS&CURT) or curtailment only (CURT) to reduce the magnitude of reverse power flows when necessary (see Section 2.3). The simulations carried out show that the BESS mechanism (with no curtailment) requires a 250.5 kWh capacity battery bank, with a maximum charging and discharging power of 134 kW and 110 kW, respectively, to keep reverse power flows within the limits for a normal operation. Since any storage capacity could be selected for the BESS&CURT based operation, this study assumes that an arbitrary storage capacity of 135 kWh is used. This value was chosen because it is the maximum limit of battery bank units that can be

put into operation in an installation, imposed by the chosen manufacturer available in the market [33]. For both BESS and BESS&CURT mechanisms it is assumed that a roundtrip efficiency of 90 % is offered by each individual battery (e.g. see Tesla Powerwall [33]). The collected results show that the equivalent aging of the distribution transformer, over the analyzed 1-year period, is similar for three operations (see Table 5). Likewise, the transformer's load and temperature profiles are identical, being presented in Figures 13 and 14 for the TAAPS operation based on BESS.

Table 5 – Equivalent aging for each scenario.

	Protection mechanism	Equivalent aging [Days]
Original	-	2.8
nZEB	-	2050
nZEB w/ TAAPS	BESS	302
	BESS&CURT	302
	CURT	302

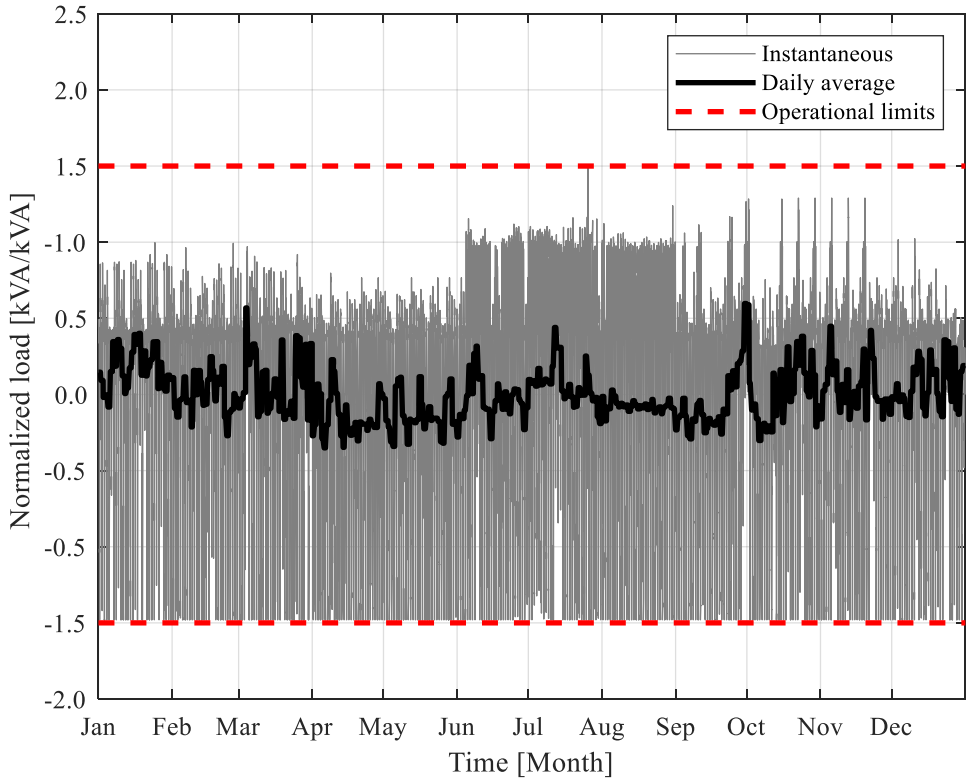

Figure 13 – Instantaneous and daily average load profile of the transformer at the nZEB condition with the TAAPS.

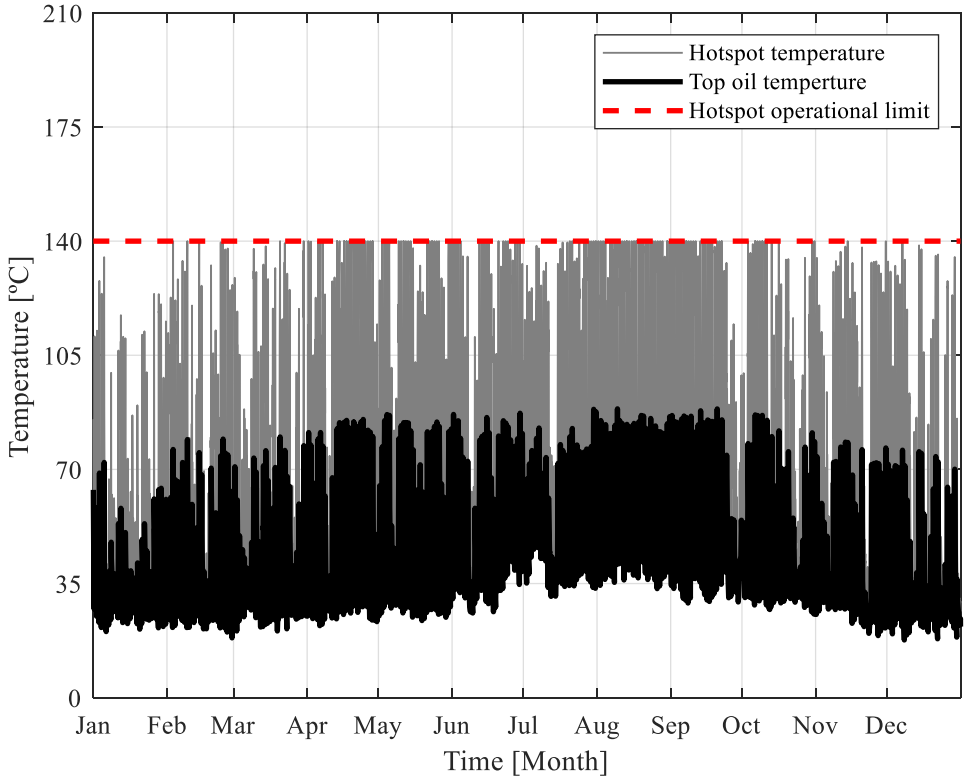

Figure 14 – Transformer temperature profiles at the nZEB condition with the TAAPS.

With the protection system, the load normal operation limit of 1.5 times the transformer's rated load is always respected, even in situations of generation surplus around noon (the instants when the aging process is mostly accelerated in the second scenario). Regarding the hotspot temperature, it does not exceed the limit of 140º. The resulting equivalent aging throughout the year is shown in Figure 15, where a reduction of 85.2 % is observed at the end of the considered 1-year period when compared to the nZEB scenario depicted in Figure 11 (from 2050 to 302 days). Therefore, the main objective of limiting transformer equivalent aging is achieved by TAAPS when considering BESS, BESS&CURT or CURT.

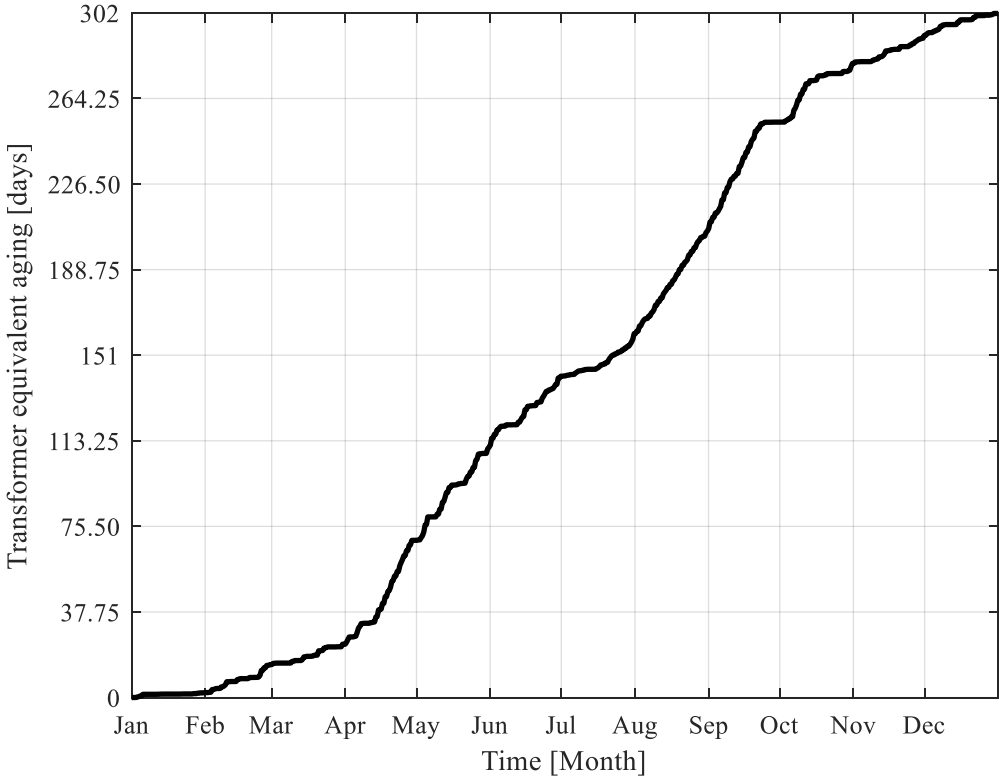

Figure 15 – Transformer equivalent aging at the nZEB condition with the TAAPS.

To better understand the TAAPS operation (only BESS) on a daily basis, Figure 16 shows the transformer's load during an arbitrary summer day. During the period with higher PV generation, the BESS is charged to avoid reverse power flows with excessive magnitude or hotspot temperatures greater than 140 ºC, as presented in Figure 17. The stored energy (which corresponds to the area between the black and grey lines, around noon) is then discharged to supply the building during the evening, when the demand is higher than the PV generation. Consequentially, there is no energy flowing through the transformer, allowing it to cool down limiting its aging process. The amount of stored energy, defined by the chosen operational limits for the admitted load and the hotspot temperature, is therefore directly related to the decreasing rate of the aging process. For this illustrative day, Figure 18 presents the resulting aging process, where the benefits introduced by the TAAPS are evident. On the original scenario, before the conversion of the DEEC building

to nZEB, the aging of the transformer on this day is equal to only 0.0013 days. After the conversion of the building to nZEB, the equivalent aging on this day equals 5.49 days, while the TAAPS operation reduces this value to an equivalent aging of 2.56 days. Despite the increase from the initial situation, after the installation of the TAAPS the aging for this day is decreased by 53.4% when compared to the second scenario, for this specific day. However, even with the TAAPS, the equivalent aging is not unitary due to the operation at hotspot temperature values higher than 110 ºC for a period too large to be compensated by the operation at lower temperatures (it is important to note that the equivalent aging is exponentially dependent on the hotspot temperature, as described by Equation 7).

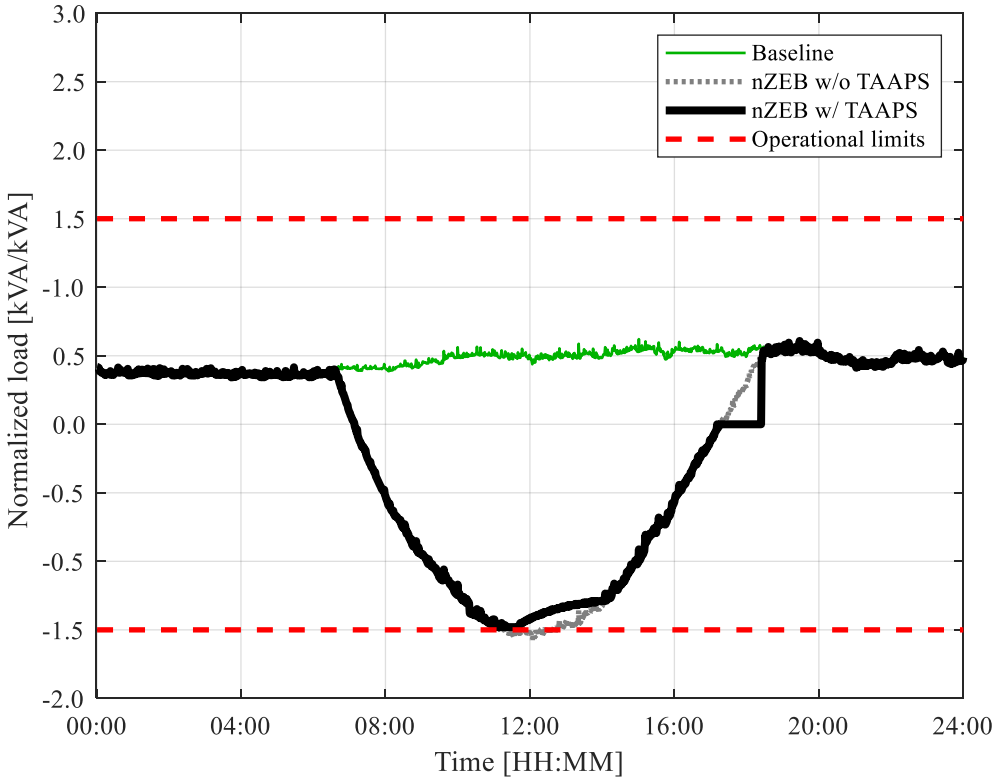

Figure 16 – Transformer load, for each scenario, on a 24-h period during a summer day, where the TAAPS operation is based on BESS.

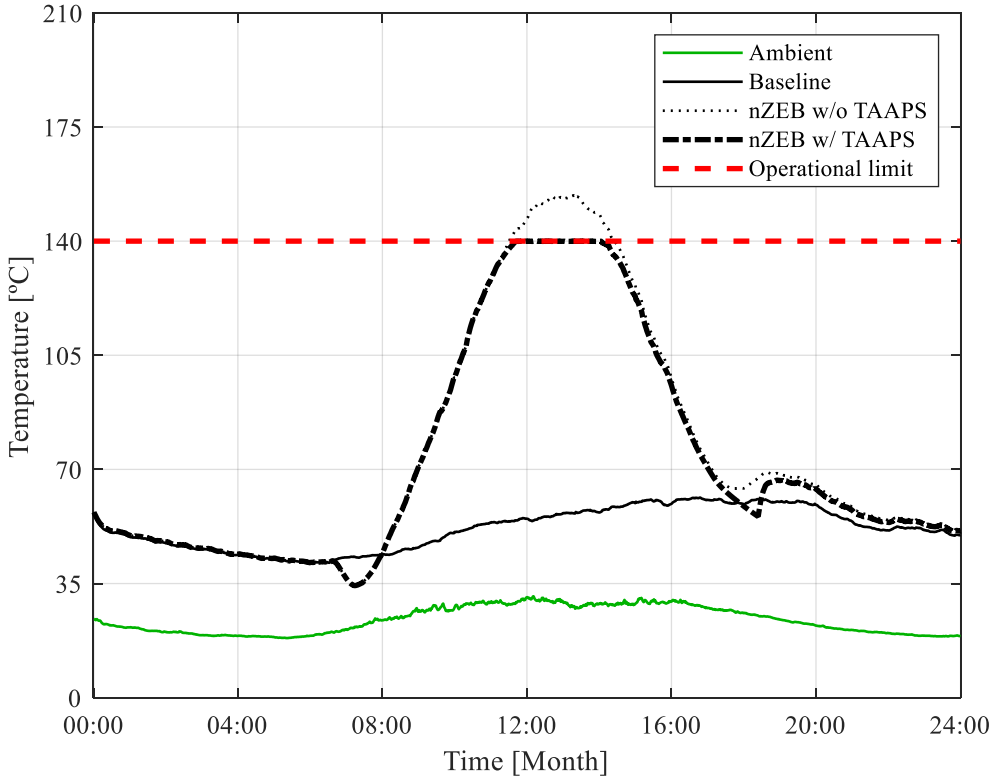

Figure 17 – Transformer hotspot temperature on a 24-h period during a summer day, where the TAAPS operation is based on BESS.

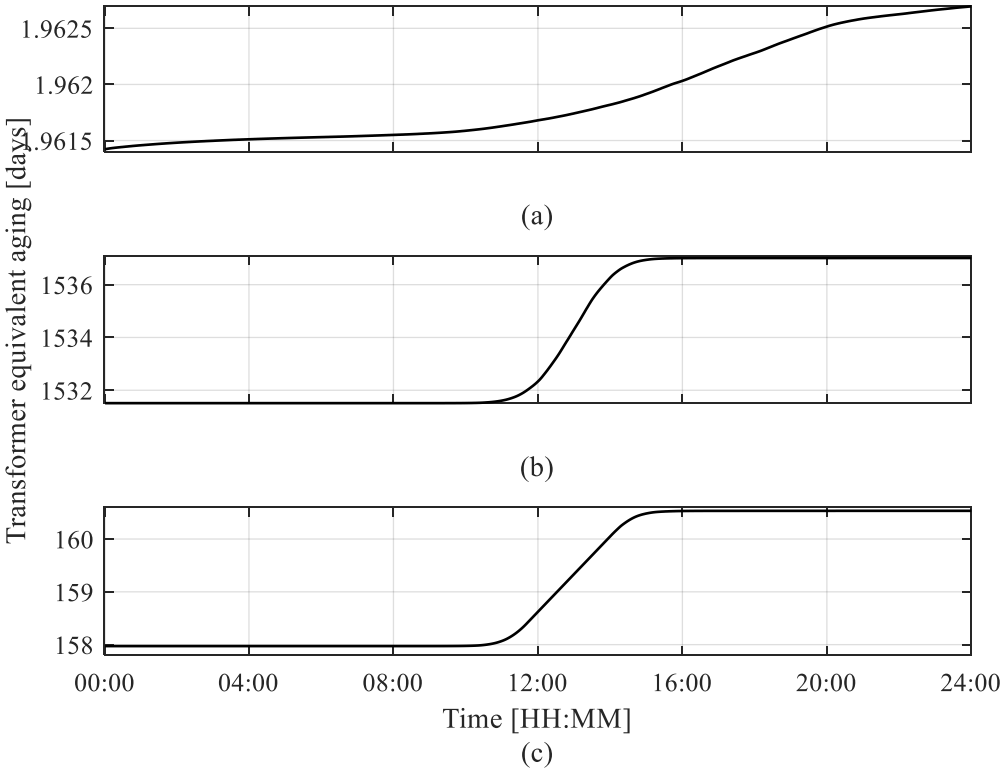

Figure 18 – Transformer aging on a 24-h period during a summer day for each scenario: (a) before the introducing PV generation; (b) at nZEB condition; (c) at nZEB condition with the TAAPS operation based on BESS.

While the presented results do not vary significantly with the selected protection mechanism (i.e. BESS, BESS&CURT or CURT), it is important to assess the relation between the storage capacity and the necessity of curtailment when the BESS&CURT is chosen. This relation is presented in Figure 18, considering the annual curtailed energy and the battery bank storage capacity for the BESS&CURT mechanism. As the storage capacity of the BESS installed decreases, the need for curtailment increases. By using the BESS&CURT mechanism, the daily curtailed energy varies every day due to the different ambient temperature and the solar irradiation conditions. As a result, for larger BESS the full storage capacity is often not used.

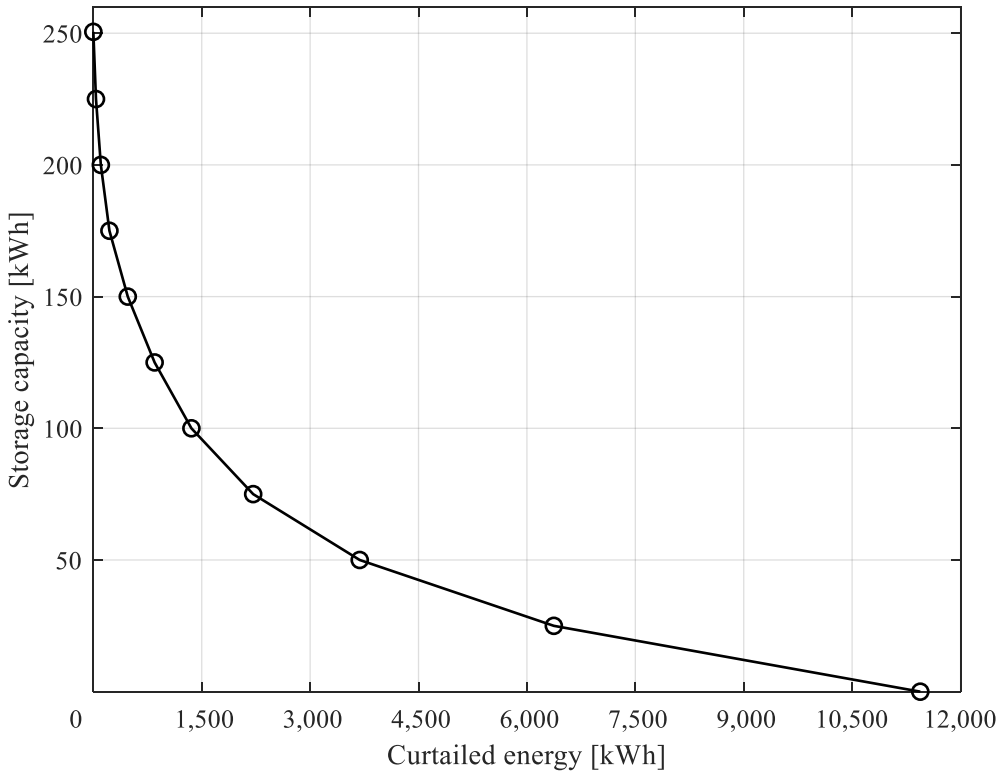

Figure 19 – Relation between Storage Capacity and needed Curtailment for the BESS&CURT mechanism.

3.4 – Economic analysis

This section provides an economic analysis for all scenarios under the Portuguese context, using the Net Present Value (NPV) computed over 10 years as quantitative metric and 2013 as the first year. Therefore, for each year, this analysis considers the cost associated to the electricity import and the revenue resulting from electricity export (this revenue is not considered for the original scenario due to the lack of local generation). Since the collected data only comprises one year, two assumptions were considered. The first one is related with the electricity demand of the building. In this case, it is assumed that the electricity demand profile of the building does not change over the 10-year period. The second one assumes that the PV system generation presents a yearly reduction of 1 %, due to the inherent elements aging.

Regarding the import costs, Portuguese market data associated to costumers supplied in MV from 2013 to 2019 [34] were used for the first seven years. As described in Table 6, the used data refer to a fixed value to be paid at each month, a value dependent on the power consumption at peak periods, a cost associated to the contracted power and the value of the Time-of-Use tariffs, which considers four different values throughout the day. All these values differ according to four different periods (Period I: from January 1st to March 31; Period II from April 1st to June 30; Period III from July 1st to September 30; and Period IV from October 1st to December 31). It is important to mention that under the Portuguese context, electricity import costs are also dependent on the consumed reactive energy. However, since the data collected comprehends only the active power, reactive energy related costs were not considered in this study. The data associated to the last three years of this economic analysis have been estimated from the available data, using a linear regression methodology.

Table 6 – Importation tariffs values from 2013 to 2019 [34].

Tariff type		**2013**	**2014**	**2015**	**2016**	**2017**	**2018**	**2019**
Fixed [€/month]		47.20	45.19	46.28	47.33	47.84	47.81	46.07
Peak hours [€/kW.month]		9.289	9.959	9.92	10.157	10.280	10.266	10.087
Contracted power [€/kW.month]		1.448	1.468	1.516	1.552	1.570	1.568	1.544
Period I and IV	Peak [€/kWh.month]	0.1252	0.1287	0.1335	0.1368	0.1384	0.1382	0.1382
	Half-peak [€/kWh.month]	0.0969	0.1004	0.1048	0.1074	0.1087	0.1085	0.1101
	Normal off-peak [€/kWh.month]	0.0644	0.0708	0.0739	0.0757	0.0767	0.0765	0.0777
	Super off-peak [€/kWh.month]	0.0586	0.0604	0.0631	0.0646	0.0654	0.0656	0.0666
Period II and III	Peak [€/kWh.month]	0.1286	0.1316	0.1364	0.1397	0.1414	0.1412	0.1408
	Half-peak [€/kWh.month]	0.0995	0.1030	0.1070	0.1096	0.1109	0.1107	0.1124
	Normal off-peak [€/kWh.month]	0.0669	0.0735	0.0765	0.0784	0.0793	0.0792	0.0791
	Super off-peak [€/kWh.month]	0.0624	0.0677	0.0703	0.0720	0.0729	0.0728	0.0728

According to the Portuguese PV self-consumption regime, the revenue resulting from generation surplus export is given by the monthly average value of the Portuguese electricity spot market multiplied by a constant equal to 0.9. Table 7 presents the values

of this market from 2013 to 2018. The values associated to the last four years of the analysis were obtained using a linear regression for each month.

Table 7 - Monthly average value of the Portuguese electricity spot market from 2013 to 2018 [35].

	2013 [€/MWh]	2014 [€/MWh]	2015 [€/MWh]	2016 [€/MWh]	2017 [€/MWh]	2018 [€/MWh]
Jan	48.53	31.47	51.82	36.39	71.52	51.63
Feb	43.74	15.39	42.47	27.35	51.39	54.98
Mar	41.70	26.20	43.22	27.70	43.95	39.75
Apr	16.08	26.36	45.49	23.50	44.18	42.66
May	43.25	42.47	45.18	24.93	47.12	55.08
Jun	41.70	51.19	54.74	38.28	50.22	58.48
Jul	51.40	48.27	59.61	40.36	48.60	61.84
Ago	48.12	49.91	55.59	41.14	47.43	64.29
Sep	50.68	58.91	51.92	43.61	49.16	71.30
Oct	51.19	55.39	49.89	52.78	56.97	65.38
Nov	42.10	46.96	51.46	56.25	59.36	62.01
Dec	62.99	47.69	52.92	60.27	59.49	61.87

Regarding the TAAPS initial investment, it is considered that BESS, BESS&CURT and CURT based operations incur on the same software and hardware related costs except from the required battery energy storage systems, whose acquisition costs should be considered. A specific cost per unit of stored energy of 531.56 €/kWh was used in this study, which is aligned with available market data [33] and supported by literature [36–39].

Table 8 summarizes the NPV for each scenario, where negative values are registered due to higher electricity import costs, even when the DEEC building is converted to nZEB. To assess the profitability of installing TAAPS on the existing nZEB, the difference between the NPVs can be used. The collected results show that TAAPS should be installed to prevent transformer replacement if the transformer to be installed and respective installation works are cheaper than €125182, €64346 and €4216 for the TAAPS operation based on BESS, BESS&CURT and CURT, respectively. Therefore, considering that a 200 kVA transformer is needed for a normal operation when the DEEC building is converted to nZEB (see Figure 10), this transformer replacement would have

513 to cost less than €4216 to make the TAAPS operation based only on curtailment not
514 profitable.

515 *Table 8 – Net present value (10 years) for each scenario.*

Scenario	Protection mechanism	NPV [€]
Original	-	- 452564
nZEB	-	- 157815
nZEB with TAAPS	BESS	- 282997
	BESS&CURT	- 222161
	CURT	- 162031

516

517 Due to the protection algorithm, which only considers the technical aspects of the thermal
518 limits of the transformer, the amount of exported energy does not differ among the BESS,
519 BESS&CURT and CURT based operations. Figure 20 shows the monthly average
520 exported energy for the 10 years period when considering the TAAPS operation based on
521 BESS. In June and July, due to higher ambient temperatures and higher electrical energy
522 needs to satisfy thermal comfort needs, there is a lower PV generation surplus.

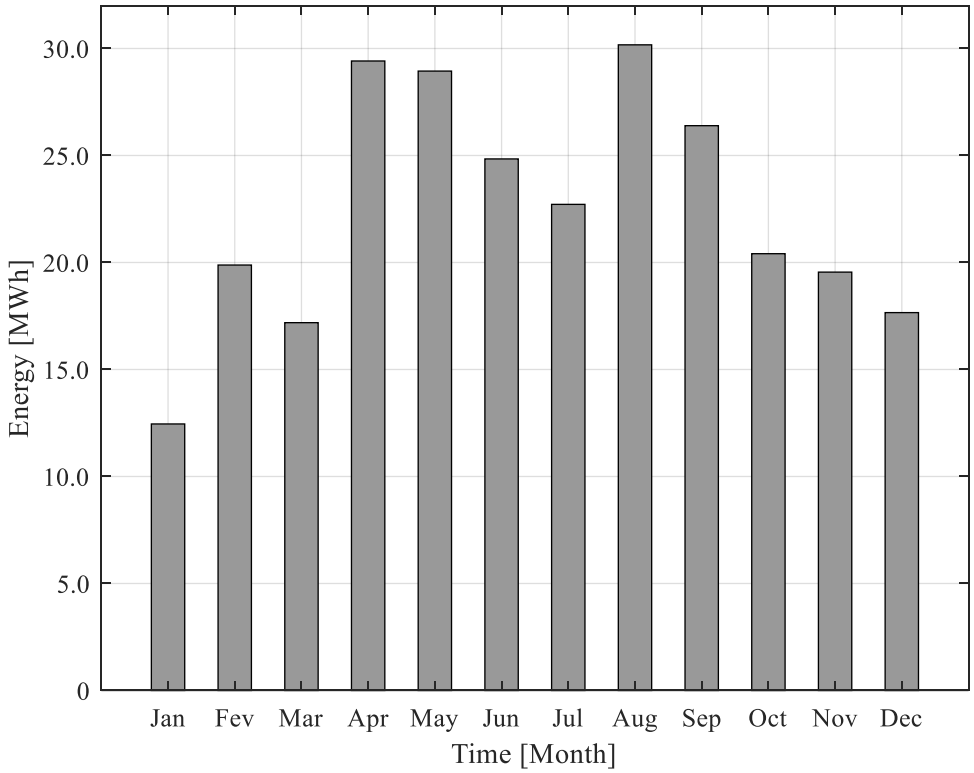

523
524 *Figure 20 – Monthly average exported energy for the 10-years TAAPS operation based*
525 *on BESS.*

Still considering the TAAPS operation, throughout the operation years, the savings from the stored energy progressively decreases as the generation capacity decreases. On the same period, the loss of revenue increases when higher amounts of energy are curtailed, which occurs by the lower BESS capacity to store electrical energy. The curtailed energy, by the very definition of curtailment, is not used by the building users, stored or exported to the distribution grid. With these factors taken into consideration, the NPV associated to the TAAPS operation was calculated without considering the replacement of the original transformer, which depends on the specific context where the building is located and therefore no costs were assumed here. For these calculations, it was considered that all TAAPS investments were made before the operation of the system and all the revenues and costs due to the operation postponed to the final of the period (one year), considering an annual discount rate of 6 %.

Despite the generated energy waste by using curtailment, strictly from the economical point of view, the CURT based operation is considered more suitable since it does not require the large initial investment associated to the acquisition of batteries. This analysis also shows that, even with the self-consumption and battery energy storage of the BESS based operation, there is still a need to import a significant amount of electricity from the grid, due to the unbalance between the peak hours of generation and consumption. Therefore, even without the initial investment, the BESS based operation would not be positive in terms of cashflow (see Figure 21). This is due to only using the available storage capacity to limit generation surplus and not exploring the storage capacity during the entire year (several days with no battery use were registered) according to the time varying electricity tariff in order to reduce import costs.

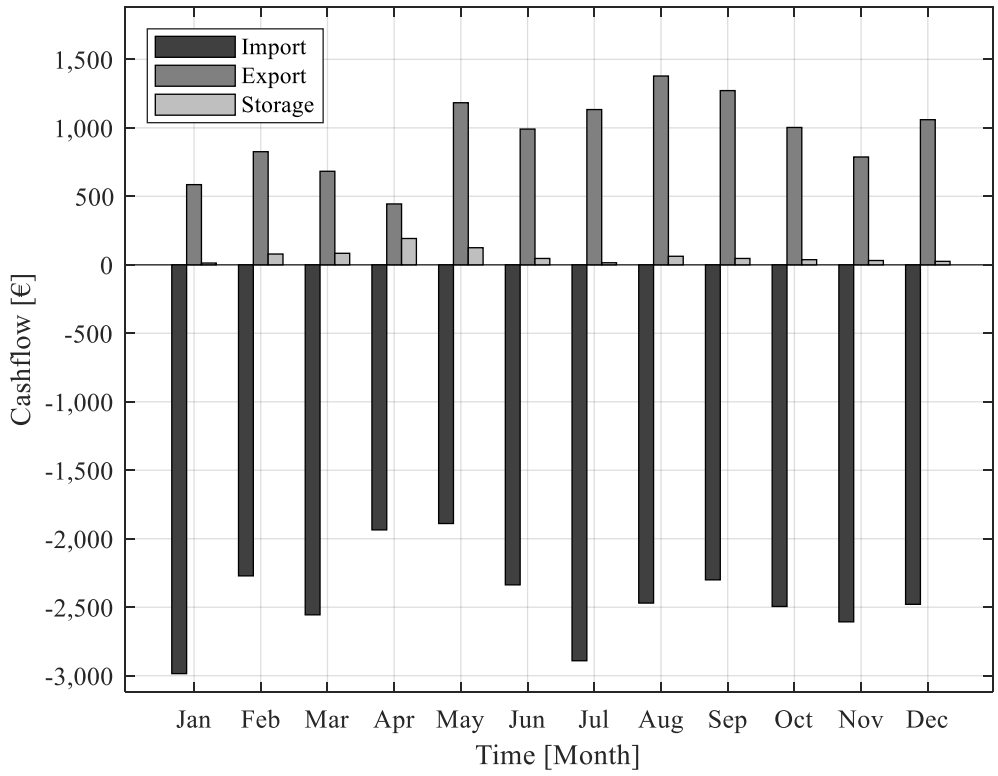

Figure 21 – Cashflow for the first year of the BESS based operation.

4 – Conclusion and Remarks

The study reported in this paper focus the impact introduced by on-site generation on large non-residential buildings distribution transformer. Additionally, this paper proposes a novel Transformer Anti-Aging Protection System, able to mitigate excessive aging using Battery Energy Storage Systems and/or generation curtailment to limit the magnitude of reserve power flows and provides an economic analysis to clarify the most suitable solution in the current Portuguese context.

The collected results show that the introduction of on-site generation in the analyzed non-residential building, due to its conversion to nZEB, introduces considerable negative impacts on transformer aging which could conduct to equipment failure. Regarding the proposed Transformer Anti-Aging Protection System, the results show that its main objective of keeping the transformer operation at normal conditions (e.g. transformer's

load lower than 1.5 times its rated load) is achieved. Economically, under the Portuguese context, this study also reveals that the operation of the proposed system, on a financial point of view, should rely on generation curtailment over energy storage since energy losses due to curtailment compensate the respective storage for latter self-consumption. As future work, one can consider the improvement of the storage discharging strategy in cases where energy storage is used to reduce the magnitude of reverse power flows. For instance, this strategy could take into consideration the tariffs in order to reduce electricity import during peak periods or the hotspot temperature associated to energy import so it could further reduce the resulting transformer aging. The contribution of other sources of energy flexibility (e.g. electric vehicles charging) should also be considered in the future as they can be controlled to increase self-consumption and therefore reduce the required energy storage capacity and/or curtailment losses while ensuring a normal transformer operation.

Acknowledgment

This work was supported by national funds through FCT – Fundação para a Ciência e a Tecnologia, under project UID/EEA/00066/2019.

References

[1] IEA, Key World Energy Statistics, 2017. https://www.iea.org/publications.
[2] NASA, Global Climate Change - VItal Signs of the Planet, (2019). https://climate.nasa.gov/ (accessed February 26, 2019).
[3] United Nations, Kyoto Protocol to the United Nations Framework Convention on Climate Change, Rev. Eur. Community Int. Environ. Law. 7 (1998) 20. http://unfccc.int/resource/docs/convkp/kpeng.pdf.
[4] United Nations Framework Convention on Climate Change, Paris Agreement, 2015. http://unfccc.int/meetings/paris_nov_2015/items/9445.php.
[5] V. Subramanyam, A. Kumar, A. Talaei, M.A.H. Mondal, Energy efficiency improvement opportunities and associated greenhouse gas abatement costs for the residential sector, Energy. 118 (2017) 795–807.

595 doi:10.1016/j.energy.2016.10.115.
596 [6] V. Subramanyam, M. Ahiduzzaman, A. Kumar, Greenhouse gas emissions
597 mitigation potential in the commercial and institutional sector, Energy Build. 140
598 (2017) 295–304. doi:10.1016/j.enbuild.2017.02.007.
599 [7] E. Commission, Buildings, (n.d.). https://ec.europa.eu/energy/en/topics/energy-
600 efficiency/energy-performance-of-buildings (accessed February 26, 2019).
601 [8] European Commission, Directive 2010/31/EU of the European Parliament and of
602 the Council of 19 May 2010 on the energy performance of buildings (recast), Off.
603 J. Eur. Union. (2010) 13–35. doi:10.3000/17252555.L_2010.153.eng.
604 [9] A. Hermelink, S. Schimschar, T. Boermans, L. Pagliano, P. Zangheri, R. Armani,
605 K. Voss, E. Musall, Towards nearly zero-energy buildings - Definition of common
606 principles under the EPBD, 2012. https://ec.europa.eu/energy/sites/ener/files.
607 [10] R.M.A. Lopes, Extending nearly Zero-Energy Buildings Load Matching
608 Improvement to Community-Level, 2017. https://run.unl.pt/handle/10362/29113.
609 [11] J. V. Paatero, P.D. Lund, Effects of large-scale photovoltaic power integration on
610 electricity distribution networks, Renew. Energy. 32 (2007) 216–234.
611 doi:10.1016/j.renene.2006.01.005.
612 [12] M.N. Kabir, Y. Mishra, G. Ledwich, Z. Xu, R.C. Bansal, Improving voltage profile
613 of residential distribution systems using rooftop PVs and Battery Energy Storage
614 systems, Appl. Energy. 134 (2014) 290–300. doi:10.1016/j.apenergy.2014.08.042.
615 [13] M. Karimi, H. Mokhlis, K. Naidu, S. Uddin, A.H.A. Bakar, Photovoltaic
616 penetration issues and impacts in distribution network – A review, Renew. Sustain.
617 Energy Rev. 53 (2016) 594–605. doi:10.1016/j.rser.2015.08.042.
618 [14] S. Hashemi, J. Østergaard, Methods and strategies for overvoltage prevention in
619 low voltage distribution systems with PV, IET Renew. Power Gener. 11 (2017)
620 205–214. doi:10.1049/iet-rpg.2016.0277.
621 [15] M. Yazdani-Asrami, M. Mirzaie, A.A. Shayegani Akmal, No-load loss calculation
622 of distribution transformers supplied by nonsinusoidal voltage using three-
623 dimensional finite element analysis, Energy. 50 (2013) 205–219.
624 doi:10.1016/j.energy.2012.09.050.
625 [16] H. Jimenez, H. Calleja, R. González, J. Huacuz, J. Lagunas, The impact of
626 photovoltaic systems on distribution transformer: A case study, Energy Convers.
627 Manag. 47 (2006) 311–321. doi:10.1016/j.enconman.2005.04.007.
628 [17] S.M.M. Agah, H. Askarian Abyaneh, Quantification of the Distribution
629 Transformer Life Extension Value of Distributed Generation, IEEE Trans. Power
630 Deliv. 26 (2011) 1820–1828. doi:10.1109/TPWRD.2011.2115257.
631 [18] A.S. Masoum, P.S. Moses, M.A.S. Masoum, A. Abu-Siada, Impact of rooftop PV
632 generation on distribution transformer and voltage profile of residential and
633 commercial networks, in: 2012 IEEE PES Innov. Smart Grid Technol., IEEE,
634 2012: pp. 1–7. doi:10.1109/ISGT.2012.6175693.
635 [19] D. Martin, S. Goodwin, O. Krause, T. Saha, The effect of PV on transformer
636 ageing: University of Queensland's experience, 2014 Australas. Univ. Power Eng.
637 Conf. AUPEC 2014 - Proc. (2014) 1–6. doi:10.1109/AUPEC.2014.6966484.
638 [20] M. Hamzeh, B. Vahidi, H. Askarian-Abyaneh, Reliability evaluation of
639 distribution transformers with high penetration of distributed generation, Int. J.
640 Electr. Power Energy Syst. 73 (2015) 163–169. doi:10.1016/j.ijepes.2015.04.013.
641 [21] M.K. Gray, W.G. Morsi, On the role of prosumers owning rooftop solar
642 photovoltaic in reducing the impact on transformer's aging due to plug-in electric
643 vehicles charging, Electr. Power Syst. Res. 143 (2017) 563–572.

644 doi:10.1016/j.epsr.2016.10.060.
645 [22] K. Kumar, G.B. Kumbhar, The effect of solar power injection on aging of a
646 distribution transformer, in: 2017 6th Int. Conf. Comput. Appl. Electr. Eng. Adv.,
647 IEEE, 2017: pp. 242–246. doi:10.1109/CERA.2017.8343334.
648 [23] A.R.A. Manito, A. Pinto, R. Zilles, Evaluation of utility transformers' lifespan with
649 different levels of grid-connected photovoltaic systems penetration, Renew.
650 Energy. 96 (2016) 700–714. doi:10.1016/j.renene.2016.05.031.
651 [24] S.A. El Batawy, S. Member, W.G. Morsi, S. Member, On the Impact of High
652 Penetration of Rooftop Solar Photovoltaics on the Aging of Distribution
653 Transformers solaires photovoltaïques sur le vieillissement des transformateurs de
654 distribution, 40 (2017) 93–100. doi:10.1109/CJECE.2017.2694698.
655 [25] H. Pezeshki, P.J. Wolfs, G. Ledwich, Impact of High PV Penetration on
656 Distribution Transformer Insulation Life, IEEE Trans. Power Deliv. 29 (2014)
657 1212–1220. doi:10.1109/TPWRD.2013.2287002.
658 [26] M.A. Awadallah, T. Xu, B. Venkatesh, B.N. Singh, On the Effects of Solar Panels
659 on Distribution Transformers, IEEE Trans. Power Deliv. 31 (2016) 1175–1185.
660 doi:10.1109/TPWRD.2015.2443715.
661 [27] K.D. McBee, Transformer Aging due to High Penetrations of PV, EV Charging,
662 and Energy Storage Applications, in: 2017 Ninth Annu. IEEE Green Technol.
663 Conf., IEEE, 2017: pp. 163–170. doi:10.1109/GreenTech.2017.30.
664 [28] S. Freitas, T. Santos, M.C. Brito, Impact of large scale PV deployment in the sizing
665 of urban distribution transformers, Renew. Energy. 119 (2018) 767–776.
666 doi:10.1016/j.renene.2017.10.096.
667 [29] R.A. Lopes, P. Magalhães, J.P. Gouveia, D. Aelenei, C. Lima, J. Martins, A case
668 study on the impact of nearly Zero-Energy Buildings on distribution transformer
669 aging, Energy. 157 (2018) 669–678. doi:10.1016/j.energy.2018.05.148.
670 [30] IEC, IEC 60076-7:2005 - Loading guide for oil-immersed power transformers,
671 2005.
672 [31] R.A. Lopes, J. Martins, D. Aelenei, C.P. Lima, A cooperative net zero energy
673 community to improve load matching, Renew. Energy. 93 (2016) 1–13.
674 doi:10.1016/j.renene.2016.02.044.
675 [32] J.A. Duffie, W.A. Beckman, Solar Engineering of Thermal Processes, 4th ed., John
676 Wiley & Sons, Inc., Hoboken, NJ, USA, 2016. doi:10.1115/1.2930068.
677 [33] Tesla, Powerwall, (n.d.). https://www.tesla.com/pt_PT/powerwall (accessed May
678 13, 2019).
679 [34] ERSE, Tarifas e Preços. http://www.erse.pt/pt/electricidade/tarifaseprecos
680 (accessed May 23, 2019).
681 [35] OMIE, Informe anual, (2015). http://www.omie.es/inicio/publicaciones/informe-
682 anual (accessed May 23, 2019).
683 [36] X. Luo, J. Wang, M. Dooner, J. Clarke, Overview of current development in
684 electrical energy storage technologies and the application potential in power
685 system operation, Appl. Energy. 137 (2015) 511–536.
686 doi:10.1016/j.apenergy.2014.09.081.
687 [37] V. Jülch, Comparison of electricity storage options using levelized cost of storage
688 (LCOS) method, Appl. Energy. 183 (2016) 1594–1606.
689 doi:10.1016/j.apenergy.2016.08.165.
690 [38] G.L. Kyriakopoulos, G. Arabatzis, Electrical energy storage systems in electricity
691 generation: Energy policies, innovative technologies, and regulatory regimes,
692 Renew. Sustain. Energy Rev. 56 (2016) 1044–1067.

693 doi:10.1016/j.rser.2015.12.046.
694 [39] P. Nikolaidis, A. Poullikkas, Cost metrics of electrical energy storage technologies
695 in potential power system operations, Sustain. Energy Technol. Assessments. 25
696 (2018) 43–59. doi:10.1016/j.seta.2017.12.001.
697